

FATIGUE AND FRACTURE RESISTANCE OF A  
WELDED BRIDGE DETAIL

R. Roberts\*, J. W. Fisher\*, G. R. Irwin\*, K. D. Boyer\*\*,  
H. Hausamann\*, G. V. Krishna\*\*, V. Morf\*\*, R. E. Slockbower\*\*,  
and J. Nishanian\*\*\*

\*Fritz Engineering Laboratory, Lehigh University, Bethlehem, PA, USA  
\*\*Formerly Fritz Engineering Laboratory, Lehigh University, Bethlehem, PA, USA  
\*\*\*Office of Research, Federal Highway Administration, Washington, DC, USA

ABSTRACT

Six large welded steel beams containing lateral attachments were fabricated from A36, A588 and A514 steels which met the 1974 AASHTO toughness specifications. These beams with their welded details were then cyclically loaded at room temperature for two million cycles at the design stress level appropriate for two million cycles. The beams were then cooled to  $-40^{\circ}\text{F}$  ( $-40^{\circ}\text{C}$ ) and lower while the cycling was continued until rapid fracture of the beams was obtained. The fracture resistance of each beam was estimated by Fracture Mechanics methodology. These results were then compared to material toughness results. The current AASHTO material specification and fatigue rules were then checked for applicability to the large beam tests. In most fracture tests the residual stresses in the beams was found to play a significant role in the fracture response. The AASHTO fatigue rules and material toughness requirements were found to be acceptable for the lateral attachments.

KEYWORDS

Fracture control, fatigue, fracture, bridges, bridge design, fatigue of weldments, beam fracture.

INTRODUCTION

The failure of the Point Pleasant Bridge (Anon. 1970) raised many questions as to the safety of steel bridges in the United States. In response to this the American Association of State Highway and Transportation Officials (AASHTO) adopted a set of material toughness requirements which in conjunction with existing AASHTO fatigue rules were believed capable of providing safe steel bridges.

The basic material toughness requirements were established in terms of the Charpy V-notch (CVN) performance of the steel at a given temperature which depended upon the lowest expected service temperature of the bridge. The utilization of the CVN test rather than other toughness measurement techniques was predicated on the familiarity of the CVN test to most engineers. A detailed discussion of the rationale behind the AASHTO material toughness requirements is provided by Barsom (1973).

The origins and technical basis for the AASHTO fatigue rules are discussed in

the work of Fisher (1977). These rules are based on the type of weld detail being considered. Each weld detail is classified so as to reflect the level of stress concentration at the detail. For a desired fatigue life, the rules provide for each detail an allowable stress range. This stress range, the difference between the maximum and minimum stress in a cycle, does not depend on material type or the maximum stress level.

To evaluate the adequacy of the AASHTO material toughness requirements and the fatigue rules a series of fatigue and fracture tests were carried out on large beams containing various weld details. This paper briefly describes the tests and test results obtained for beams containing lateral attachments, an AASHTO fatigue class "E" welded detail. Roberts and co-workers (1977) provide a more detailed discussion of the results discussed in this paper and test results for other weld details.

Test Program

A test program was designed to evaluate the ability of the 1974 AASHTO fatigue rules and material toughness requirements to provide a satisfactory fatigue life at the lowest expected service temperature. To this end, fatigue and fracture tests were carried out on six large beams which contained lateral attachments. Two beams were made of ASTM type A36 steel, two beams of type A588 steel and two beams of type A514 steel. Details of these beams are given in Fig. 1. Here it can be seen that two types of lateral attachments were employed. One was groove welded to the beam flange tip while the other was lapped and fillet welded to the inner flange surface. This provided two welded details of each kind on the tension flange. The use of this configuration at both the top and bottom of the beam provided symmetry. This is important both in terms of the test loading and also the final analytical analysis of the test results.

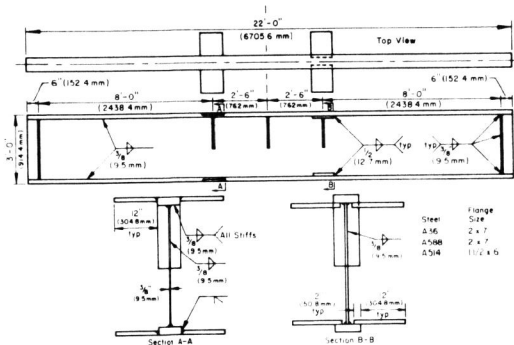


Fig. 1. Lateral attachment details.

For the purpose of these tests it was assumed that the lowest expected service temperature would be -40°F (-40°C). As such the materials were purchased to conform to the AASHTO toughness requirements for this temperature. The nominal properties of the flange materials are given in Table 1.

The lateral attachment details studied in this program correspond to an AASHTO category "E" fatigue detail. For this classification the stress range ( $\sigma_r$ ) is not to exceed 8 KSI (56.2 MPa) for two million cycles of life. Furthermore the maximum stress in the tension flange is limited to 55 percent of the yield strength ( $\sigma_{ys}$ ) of the flange material.

TABLE 1 Nominal Flange Properties

| Material | Flange Thickness in. (mm) | Yield Strength KSI (MPa) | Ultimate Strength KSI (MPa) | NDT °F (°C) |
|----------|---------------------------|--------------------------|-----------------------------|-------------|
| A36      | 2 (50.8)                  | 44.0 (303)               | 70.0 (483)                  | - 5 (-21)   |
| A588     | 2 (50.8)                  | 56.5 (390)               | 78.5 (541)                  | 5 (-15)     |
| A514     | 1.5 (38.1)                | 125.1 (863)              | 134.2 (925)                 | -85 (-65)   |

To obtain the desired maximum stress and stress range a test setup as shown in Fig. 2 was used. Due to limitation on hydraulic ram capacity the maximum stress and stress range requirements could only be obtained simultaneously with rams P2 for the A36 material. For the A588 and A514 materials an additional static ram, P1, was used to obtain the maximum stress. Rams P2 were used to produce the stress range. In all tests the cyclic load was applied at a rate of 260 cycles per minute. This corresponds to approximately the loading rate encountered in main load carrying members in bridges. Cold N2 gas was used in conjunction with the insulated box shown in Fig. 2 to produce the desired temperature at the test detail. If two details were tested together then two cooling boxes were used.

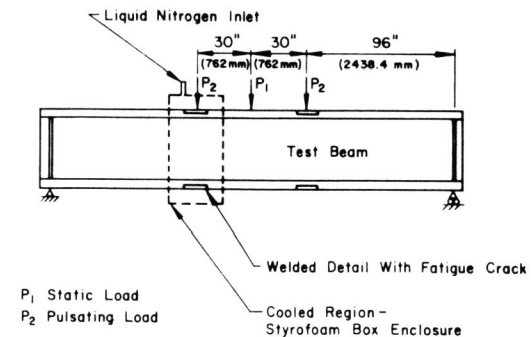


Fig. 2. Test configuration.

Each beam was cyclically loaded for two million cycles or until the fatigue cracks became a possible critical size, whichever occurred first. At this point each section of the beam containing the details was cooled to -40°F (-40°C). The beam was then cycled for at least one-half hour between a maximum stress of 0.55  $\sigma_{ys}$  and a minimum stress of 0.55  $\sigma_{ys} - \sigma_r$ . If no visible fatigue cracks existed after two million cycles the fracture test was discontinued and further fatigue cycles applied at room temperature to enlarge the crack.

If there was a possible critical fatigue crack at the beginning of the first fracture test and no fracture occurred in the first one-half hour, either an extended test at -40°F (-40°C) was run or the temperature was dropped below -40°F (-40°C). This temperature drop was done slowly to obtain accurate surface temperature readings. This extended test was continued until fracture or until the liquid nitrogen supply was depleted. If there was no fracture, the beam was again fatigue cycled at room temperature to increase the crack size. The next low temperature test was run on the detail with the largest fatigue crack after the

crack had grown a predetermined amount. This fatigue and fracture test sequence was continued until a fracture occurred.

It was initially intended to fatigue cycle between the same minimum and maximum stress limits as in the fracture tests. However, this was discontinued after three tests for several reasons. First, operating the constant load jack under cyclic deflection for such extended periods caused excessive wear and heating which caused damage to the hydraulic ram. In addition, it appeared that fatigue cracking at room temperature at the limit of allowable stress could cause effects known as "warm prestressing" (Brothers and Yukawa, 1962). Such effects, if present, could result in a greater apparent fracture resistant condition. The earlier studies by Fisher and co-workers (1970) have demonstrated that the level of maximum stress had no appreciable effect on fatigue. Hence, in subsequent tests, the cyclic stress range was applied at a lower level of maximum stress.

Along with the material tests reported in Table 1 a series of fracture toughness measurements were conducted on the flange material as a function of temperature. Three point bend specimens were used for these tests. The tests were carried out at two loading rates; dynamic and what is termed here static. The dynamic loading tests produced failure times on the order of 0.001 seconds in the three point bend specimens while the static tests produced times of the order of 1 second. The static tests have loading rates comparable to bridge loading rates. The results of these toughness tests are presented in the following section of this paper. Roberts and co-workers (1977) give more detail of the tests.

To assist in the analysis of the beam tests a series of studies were undertaken to determine the residual stresses in the beams. The residual stresses due to flame cutting during preparation of the beam flanges and the welding of the beams and lateral attachments were determined. Again, Roberts and co-workers (1977) provide more details of these studies.

TEST RESULTS

The results of the beam tests are summarized in Fig. 3. Here the various parameters at fracture are listed.  $\sigma_{max}$  represents the maximum fiber stress at fracture.  $\sigma_{yd}$  is the dynamic yield strength for the material at both the failure loading rate and temperature.  $T_c$  is the failure temperature.  $K_c$  represents the estimate of the stress intensity level in the beam at failure.  $a$  and  $r_y$  are the estimates of the crack size as an edge crack in the flange and the plastic zone size at failure respectively.  $N$  is the number of load cycles at failure.

The results of the fatigue tests are shown in Fig. 4. Here the cycles at which cracking was first detected is shown along with the cycles at failure. These values are superimposed on the AASHTO category "E" design curve.

All the flange cracks in the lateral attachment details were large edge cracks at fracture. This tended to simplify the calculations of the stress intensity factor. However, since the plates were flame cut and the beams and details were welded, a rather complex residual stress pattern was present at the detail cross-section. Therefore several steps were used to estimate the value of the stress intensity factor,  $K$ .

By the method of superposition the following contributions were used to determine the magnitude of  $K$ . The primary contribution was from the applied stresses at failure. A secondary contribution was from the residual stresses at the detail cross-section. The residual stresses at the cracked section resulted from two contributions. One contribution to  $K$  was from the residual stresses at a typical cross-section of the welded beam. These stresses were caused by the web-to-flange

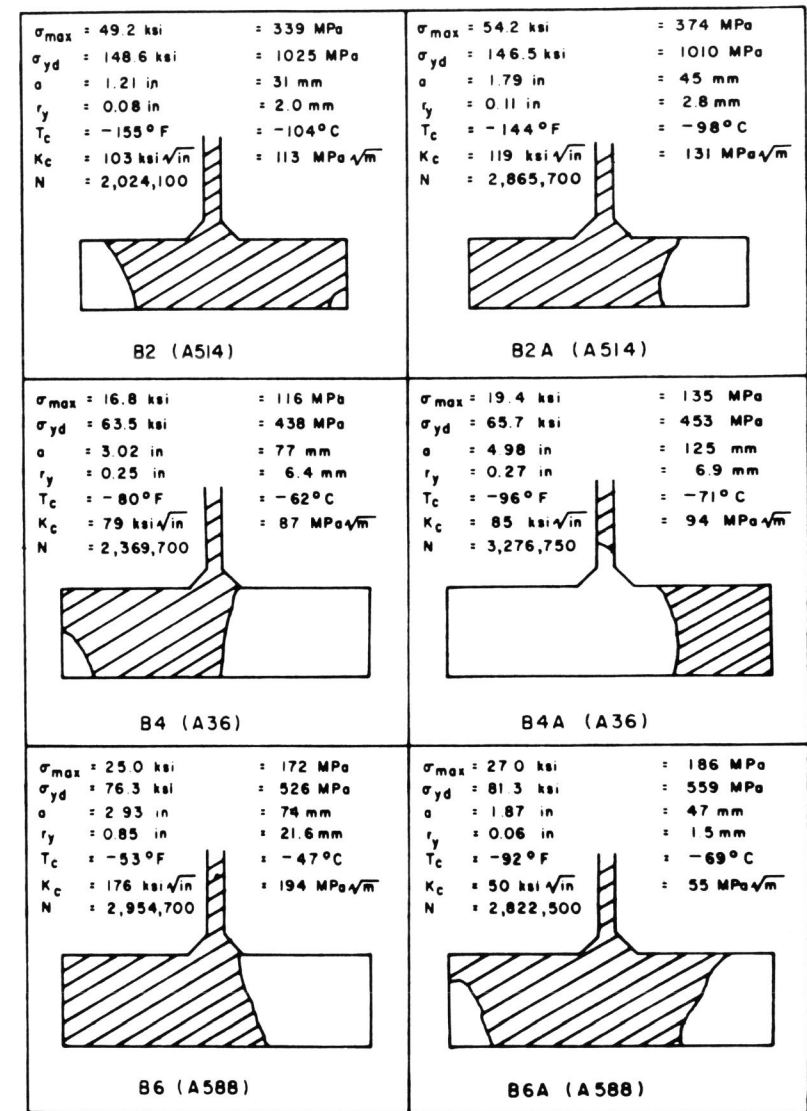


Fig. 3. Beam fracture and fatigue results.

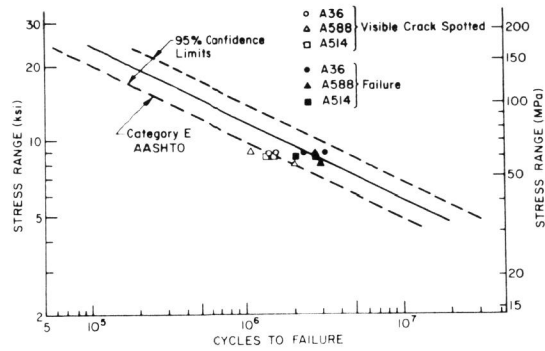


Fig. 4. Fatigue curve and results.

welds and the flame cut plate edges. The other contribution was due to the residual stresses caused by the local detail welds.

In one case, beam B4A, the flange edge crack grew through the web-to-flange welds. The fatigue crack growth continued in two directions, upward into the web and across the flange. Therefore, when estimating the stress intensity, the web interaction had to be considered as well. The web restrained the large flange crack from opening. Thus the contribution of this web restraint to the stress intensity estimate was negative.

The value of K was found to be the sum of the four terms in Eq. 1

$$K = K_{AS} + K_{RS} + K_{LW} + K_{WR} \quad (1)$$

The subscripts  $K_{ij}$  in Eq. 1 are the various contributions to the critical stress intensity. These include contributions from the applied stress,  $K_{AS}$ ; the residual stress caused by flame cut edges and web-to-flange welds,  $K_{RS}$ ; the residual stress caused by local detail welds,  $K_{LW}$ ; and the web restraint of the flange for beam B4A,  $K_{WR}$ .

Plastic-zone corrections were made by using the following plane stress relationship.

$$r_y = 0.16(K/\sigma_{ys})^2 \quad (2)$$

Using an interactive process between Eqs. 1 and 2 values of K were obtained. These values of K are given in Fig. 3. They are also shown on Figs. 5, 6, and 7. Here both the K level due only to the applied stress  $K_{AS}$  and the complete K value from eq. (1) are shown. Figs. 5, 6 and 7 also show the results of the dynamic and static material toughness tests as well as an estimate of the dynamic toughness as proposed by Barsom (1973). As with the test program a more complete description of the test results and analysis presented here can be found in the work of Roberts and co-workers (1977).

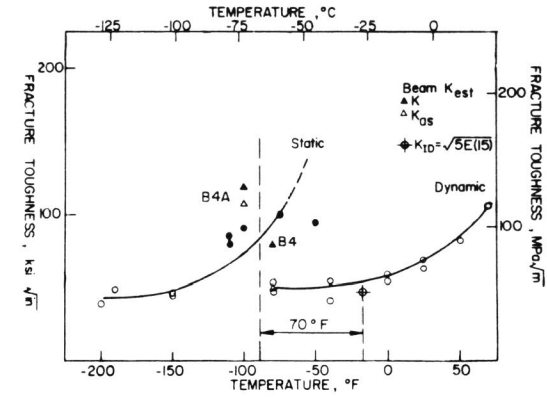


Fig. 5. A36 fracture results.

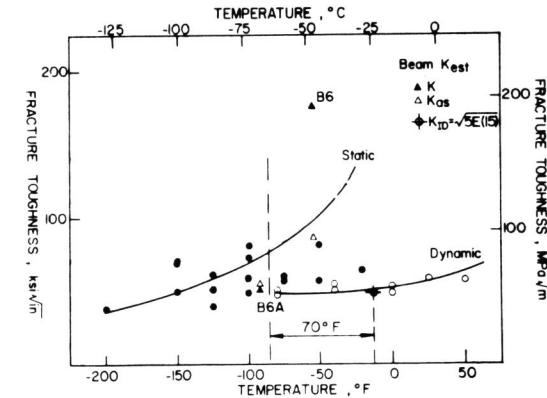


Fig. 6. A588 fracture results.

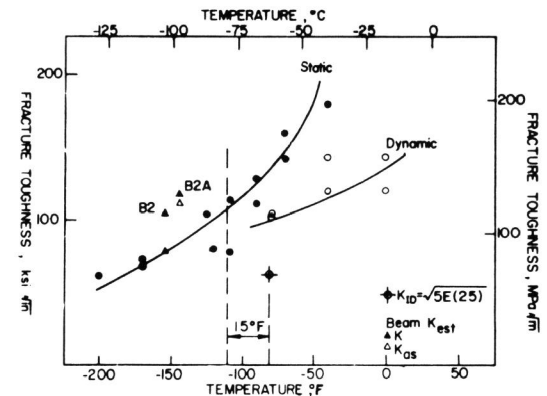


Fig. 7. A514 fracture results.

## COMMENTS ON TEST RESULTS

Space limitations prevent an extensive discussion of the tests and test results presented in this paper. However it is fair to observe for the type and size of the welded details and beams studied that the AASHTO "E" fatigue classification provides an adequate description of the fatigue life. In addition the beam fracture tests are best represented by the one second K results. This is reasonable since the loading rates between these two are approximately the same. The AASHTO material toughness requirements which were based on being able to predict the dynamic K curve from CVN results and that the dynamic and one second K curves are separated by a predictable temperature difference is also reasonable. Figures 5, 6 and 7 show both the predicted  $K_{I_d}$  level and the temperature shift. The data are in good agreement with the predictions. As a last point, it is clear from the results that the residual stresses due to welding, etc. can play a major role in the fracture behavior of a welded detail.

## ACKNOWLEDGEMENTS

The authors would like to express their thanks to the Office of Research of the Federal Highway Administration for the support of this work at the Fritz Engineering Laboratory, Lehigh University. Thanks are due to all of the staff in Fritz Lab and in particular R. R. Dales, H. T. Sutherland, R. Grimes, R. N. Sopko, J. M. Gera, D. Wiltraut and R. Troxell.

## REFERENCES

- Anon. (1970). "Collapse of U.S. 35 Highway Bridge, Point Pleasant, West Virginia, December 15, 1967", National Transportation Report No. NTSB-HAR-71-1.
- Barsom, J. M. (February 1973). "Toughness Criteria for Bridge Steels", Tech. Report No. 5 for AISI Project 168.
- Brothers, A. J. and S. Yukawa (January 1962). "The Effect of Warm Prestressing on Notch Fracture Strength", Paper No. 62-Met-1, ASME Headquarters.
- Fisher, J. W., K. H. Frank, M. A. Hirt, and B. M. McNamee (1970). "Effects of Weldments on the Fatigue Strength of Steel Beams", NCHRP Report No. 102, Highway Research Board, National Academy of Science - National Research Council, Washington DC.
- Fisher, J. W. (1977). "Bridge Fatigue Guide-Design and Details", pub. AISC, NY, NY.
- Roberts, R., J. W. Fisher, G. R. Irwin, K. D. Boyer, H. Hausmann, G. V. Krishna, V. Morf and R. E. Slockbower (1977). "Determination of Tolerable Flaw Sizes in Full Size Welded Bridge Details", FHWA Report No. FHWA-RD-77-170.